Negative Potentials Across Biological Membranes Promote Fusion by Class II and Class III Viral Proteins

Ruben M. Markosyan and Fredric S. Cohen

Department of Molecular Biophysics and Physiology, Rush University Medical Center, Chicago, IL 60612

Voltage was investigated as a factor in the fusion of virions. Virions, pseudotyped with a class II, SFV E1 or VEEV E, or a class III protein, VSV G, were prepared with GFP within the core and a fluorescent lipid. This allowed both hemifusion and fusion to be monitored. Voltage clamping the target cell showed that fusion is promoted by a negative potential and hindered by a positive potential. Hemifusion occurred independent of polarity. Lipid dye movement, in the absence of content mixing, ceased before complete transfer for positive potentials, indicating that reversion of hemifused membranes into two distinct membranes is responsible for voltage dependence and inhibition of fusion. Content mixing quickly followed lipid dye transfer for a negative potential, providing a direct demonstration that hemifusion induced by class II and class III viral proteins is a functional intermediate of fusion. In the hemifused state, virions that fused exhibited slower lipid transfer than did nonfusing virions. All viruses with class II or III fusion proteins may utilize voltage to achieve infection.

INTRODUCTION

Each enveloped virus has one or more specific proteins responsible for fusion with a plasma membrane or intracellular membrane. The creation of a fusion pore allows the virus to pass its genome into cell cytosol. All viral fusion proteins of known structure fall into one of three classes, based on structural similarities (Harrison, 2008; White *et al.*, 2008). For each class, specific triggers induce the conformational changes that lead to fusion. Class I viral fusion proteins, composed of three identical monomers, fold into a trimer of hairpins, known as a six-helix bundle, in the final fusion state (Skehel and Wiley, 1998). Class II viral fusion proteins are structurally quite distinct from class I proteins. They do not fold into bundles. Rather, they resort to form homotrimers consisting of fusion subunits from three separate proteins. Homotrimers undergo further conformational changes to induce fusion (Kielian and Rey, 2006). The three-dimensional structures of three different class II proteins have been determined before fusion (Rey *et al.*, 1995; Lescar *et al.*, 2001; Modis *et al.*, 2003) and after fusion (Bressanelli *et al.*, 2004; Gibbons *et al.*, 2004; Modis *et al.*, 2004). The three-dimensional structure of the class III fusion protein of vesicular stomatitis virus (VSV G) has been crystallographically determined in both its prefusion (Roche *et al.*, 2007) and postfusion states (Roche *et al.*, 2006). The postfusion structures of the class III fusion proteins from baculovirus (Kadlec *et al.*, 2008), herpes simplex virus type 1 (Heldwein *et al.*, 2006), and Epstein-Barr virus (Backovic *et al.*, 2009) have also been determined. The structures of all class III fusion proteins are similar to each other.

All classes of viral fusion proteins utilize common key intermediates on the way to fusion (Zaitseva *et al.*, 2005), and

all appear to proceed through hemifusion (Yoon *et al.*, 2006; Lamb and Jardetzky, 2007; Melikyan, 2008). However, in view of their structural differences, one would expect each class to exhibit some central phenotypes not exhibited by proteins of the other two classes.

The fusion protein of Semliki Forest virus (SFV), E1/E2, is prototypic of class II viral fusion proteins. We have previously shown that for effector cells expressing E1/E2, cell-cell fusion is voltage-dependent and is inhibited by a transpositive potential across the target cell (Markosyan *et al.*, 2007). In order for this finding to be of biological significance, the mechanism of voltage dependence for cell–cell fusion would have to extend to fusion of virus to cells. Furthermore, voltage dependence would have to apply to class II fusion proteins in general for that dependence to be of broad consequence. In this study we demonstrate that voltage dependence does in fact hold for virus-cell fusion mediated by SFV E1/E2, and the phenomenon extends to other class II and class III fusion proteins.

MATERIALS AND METHODS

Cells, Reagents, and Plasmids

Human embryonic kidney (HEK) 293 T-cells were obtained from ATCC (Manassas, VA) and maintained in DMEM (GIBCO-BRL, Gaithersburg, MD) supplemented with 10% Cosmic Calf Serum (Hyclone Laboratories, Logan, UT), 1% penicillin/streptomycin, 1% L-glutamine, and 100 μg/ml genicitin. HAb2 cells were grown in the same medium as HEK 293T cells, except genicitin was omitted. Huh7.5 cells were provided by Dr. C. Rice (Rockefeller University, New York, NY) and grown in DMEM supplemented with 10% fetal bovine serum (Hyclone Laboratories), 1% nonessential amino acids, and 1% penicillin/streptomycin. Poly-L-lysine, chlorpromazine (CPZ), and *n*-propyl gallate were purchased from Sigma Chemical Co. (St. Louis, MO). The fluorescent lipophilic dye, DiD, was purchased from Invitrogen (Carlsbad, CA).

Vectors expressing murine leukemia virus (MLV) Gag-Pol, and Gag-green fluorescent protein (GFP) were kindly provided by Dr. W. Mothes (Yale University, New Haven, CT). The SFV-pCB3-wt vector to express SFV E1/E2 was provided by Dr. M. Kielian (Albert Einstein College of Medicine, Bronx, NY); the pCDNA VEEd5 2 vector for VEEV E was provided by Dr. R. Davey (University of Texas Medical Branch, Galveston, TX); pHEF-VSVG was provided by the National Institutes of Health (NIH) AIDS Research and Reference Reagent Program.

Electrical Measurements of Cell–Cell Fusion

As effector cells, we transfected HEK 293T cells by a standard calcium phosphate method to express SFV E1/E2, Venezuelan Encephalitis Virus (VEEV E), or Vesicular Stomatitis Virus (VSV G) (Samsonov *et al.,* 2002). HAb2 cells were used as the target for the SFV and VEEV effector cells. Huh-7.5 cells, a human hepatoma cell line (Blight *et al.,* 2003), were used as target cells for VSV G. Effector cells were loaded with CaAM (1.3 μM); target cells were not labeled. They were thus easily distinguishable by fluorescence. Effector and target cells were mixed and placed into the experimental chamber. The bathing solution was (in mM) 150 *N*-methylglucamine aspartate, 5 MgCl$_2$, and 2 Cs-HEPES, pH 7.2. A target cell bound to a single effector cell was identified and patch clamped (Axopatch 200A, Axon Instruments, Foster City, CA) in whole cell configuration; voltage was set at either −40 or +40 mV, and fusion pore formation and growth were determined by capacitance measurements as previously described (Markosyan *et al.,* 2007). Fusion between selected effector and target cell pairs was triggered by using a closely positioned micropipette to locally apply a small volume of an acidic solution (pH 5.7) for 1 min around the cell pair. This micropipette contained four separate channels (150-μm diameter for the entire pipette; Bioscience Tools, San Diego, CA), allowing up to four different solutions to be applied to the selected cells.) Using a focused IR laser, fusion was triggered by quickly raising temperature to 32°C for SFV E1/E2 and 37°C for VEEV E and VSV G (see section *Virus-Cell Fusion* for temperature-control details).

Determination of Infectivity

To optimize the choice of target cell for each type of pseudovirus, infectivity titers were determined for several different target cells. For infectivity measurements, pseudovirus was prepared by a standard calcium phosphate method, transfecting 293T cells with a plasmid containing the gene for the fusion protein of SFV, VEEV, or VSV and a plasmid containing a human immunodeficiency virus (HIV) gene in which a firefly luciferase gene was placed in the *nef* position as described (Connor *et al.,* 1995; He *et al.,* 1995; HIV luc, obtained from the NIH AIDS Research and Reference Reagent Program). The two plasmids were added in a 1:1 ratio, 3 μg of each, to the cells in 35-mm dishes. Two days after transfection, the media (which contained the pseudotyped virions) were collected, diluted 1:10, and added to target cells. After allowing infection to proceed for 2 d, cells were lysed, and luciferase activity was measured using a Luciferase Assay System (Promega, Madison, WI) and a plate reader (Wallac 1420 multilabel counter, Perkin Elmer-Cetus, Boston, MA). For each of the three fusion proteins, the type of target cell that exhibited the highest luciferase activity was used for the study of voltage dependence of fusion of pseudovirus to cells.

Preparation of Virus for Fusion Experiments

Pseudotyped viral particles were prepared with either SFV E1/E2, VEEV E, or VSV G as the fusion protein within the envelope, and with MLV Gag-Pol plus Gag-GFP as the core. Explicitly, these pseudovirions were prepared by co-transfecting, with a calcium phosphate method, 293T cells (60–70% confluent in 10-cm culture dishes) with MLV Gag-Pol (18.5 μg), MLV Gag-GFP (6.25 μg), and the plasmid containing a fusion protein (25 μg). [MLV Gag-GFP is cleaved, within the pseudovirus, into the smaller (~37 kDa) nucleocapsid-GFP (Markosyan *et al.,* 2005; Miyauchi *et al.,* 2009).] One day after transfection, the membranes of the 293T cells were labeled with DiD, a fluorescent lipid, by incubating the cells for 3 h at 37°C in Opti-MEM (GIBCO-BRL) containing 2.5 μM DiD. The cells were washed and returned to their regular growth media. On the second day of transfection, the media were collected, centrifuged, and passed through a 0.45-μm filter. This material was separated into small aliquots and stored at −80°C. Each aliquot was thawed only once. For typical SFV E1/E2 and VSV G viral preparations, ~30% of the labeled virions were double-labeled; the other 70% of the fluorescent particles displayed only one of the dyes. For VEEV E, ~15–20% of the virions were double-labeled.

Virus-Cell Fusion

Strategies and procedures similar to those previously described were used to monitor fusion of pseudovirions to target cells (Markosyan *et al.,* 2005). Pseudoviruses containing the desired fusion protein, DiD within the envelope, and a GFP-tagged MLV Gag core were adhered to polylysine-coated cover slips by a 2-h spinoculation at 4°C. After washing off unbound virus, target cells were added and allowed to adhere on top of the pseudovirions at 15°C for ~30 min. Typically, each cell was in contact with ~5–10 virions that were labeled by both DiD and GFP. This arrangement immobilizes the pseudovirions and places them within a single plane of focus, allowing unambiguous identification of individual virions and their fusion. A coverslip was rested upon heat-adsorbing (i.e., IR adsorbing) glass that formed the bottom of the experimental chamber. The chamber was placed on the stage of the microscope. The solution within the experimental chamber was maintained at 12°C by Peltier control (20/20 Technology, Wilmington, NC). It consisted of (in mM) 150 *N*-methylglucamine aspartate, 5 MgCl$_2$, 2 Cs-HEPES (pH 7.2), and 1 *n*-propyl gallate in order to reduce photobleaching. Patch pipettes were filled (in mM) with 155 Cs glutamate, 5 MgCl$_2$, 5 1,2-bis(2-aminophenoxy)ethane-*N,N,N,N*-tetraacetic acid, and 10 Cs HEPES (pH 7.4). A 30-s pulse of a pH 5.7 solution (also maintained at ~12°C) was delivered, through one channel of the four-channel pipette, immediately above the cells. By this means, the neutral pH solution was transiently displaced by an acidic one. Fusion was triggered by illuminating the cells with an IR laser. As described (Melikyan *et al.,* 2000a), the laser illuminated an ~300-μm-diameter region of the heat-adsorbing glass and thereby raised the temperature of the solution surrounding the cells of interest. Through computer-controlled feedback, temperature was raised to 37°C within 2 s, as measured by an immersed miniature thermistor. We define time = 0 as the moment the temperature reached 37°C and refer to this time as the moment of fusion activation.

Virus-cell fusion was visualized with a laser scanning confocal Fluoview 300 microscope (Olympus America, Melville, NY), using an UPlanApo 60×/1.20 NA water-immersion objective. Gag-GFP and DiD were excited simultaneously with a 488-nm argon and a 632-nm HeNe laser, respectively. Images were collected at 10 s/frame and later were analyzed offline. All cell-bound fluorescent particles were visually inspected, and virions that were labeled by both fluorescent dyes were analyzed. Virions that fused (i.e., released DiD and GFP), only hemifused (i.e., released only DiD), or did not respond to a manipulation were separated into groups of interest. For pseudovirus containing the fusion protein of SFV, we used HEK 293T cells (rather than HAb2 cells as in cell–cell fusion) as target; for virus containing the fusion protein of VEEV and VSV, Huh-7.5 cells were used as target. Lower extents of cell–cell fusion and pseudovirus-cell fusion occurred for VEEV E. Expression levels of this fusion protein may be lower than those for SFV E1/E2 and VSV G.

Creating the Cold-arrested Stage

The fusion intermediate of CAS (cold arrested stage) was created by locally applying a pH 5.7 solution around cells (bound to virions) for 30 s at 12°C, followed by a reneutralization to pH 7.4, also at 12°C. After creating CAS, conditions were altered at varied times, as indicated. The alterations were raising of temperature to 37°C to induce fusion, adding CPZ, and changing the polarity of the holding potential across the target cell membrane. CPZ was locally applied to the cells of interest through a channel of the pipette.

Statistical Analysis

Histograms of DiD spread under different conditions (see Figure 5) were compared using a χ^2-analysis. For each of the 12 histograms (three viruses, four histograms per virus, each displaying hemifusion or fusion for +40 or −40 mV), the first 15 time frames contained almost all the events and these frames were used for comparisons. To compare two different histograms, a 2×15 table (two conditions, 15 time frames) was constructed and the χ^2 value was calculated. A Holm-Bonferroni test was applied (to avoid biases that would otherwise be introduced because multiple pairs of histograms were compared) to obtain the statistical significance, p, at which the null hypothesis could be rejected. The null hypothesis was always taken as statistical equivalence of two histograms and was only rejected if p < 0.05.

Time courses for DiD spread from individual virions at +40 and −40 mV were compared by using the mean fluorescence profiles of individual virions. Each profile was generated by first aligning, for each virus and condition, the zero time points, defined as the last frame before commencement of the decrease in fluorescence. For each type of virion that hemifused, the aligned fluorescence intensities of individual virions were averaged over the first 18 frames to yield the fluorescence profile. For SFV E1/E2 and VSV G, the first 50 virions, as arranged chronologically, that hemifused for each voltage were used to generate the profile. The data set was smaller for VEEV E at positive potentials, and here all 44 hemifused virions were used for the analysis. To compare a +40 and −40 mV fluorescence profile, a t test was applied to pairs of points at each time, employing a Holm-Bonferroni procedure to provide a multicomparison correction. The 0.05% confidence interval for the mean difference between the time profiles was calculated. All statistical analyses were performed with MatLab 7.0.1 (MathWorks, Natick, MA).

RESULTS

Cell–Cell Fusion Induced by Class II and Class III Proteins Exhibits Voltage Dependence

Effector and target cells were bound together at 4°C, and a target cell was voltage-clamped into the whole cell configuration. The voltage of the target cells were held at either −40 or +40 mV, and pore formation and pore growth were monitored using capacitance measurements. We previously reported that for effector cells expressing class I fusion proteins [either influenza hemagglutinin (HA), avian Sarcoma and Leukosis Virus (ASLV) Env, or HIV Env], the probability of fusion pore formation and the rate of pore growth was independent of the
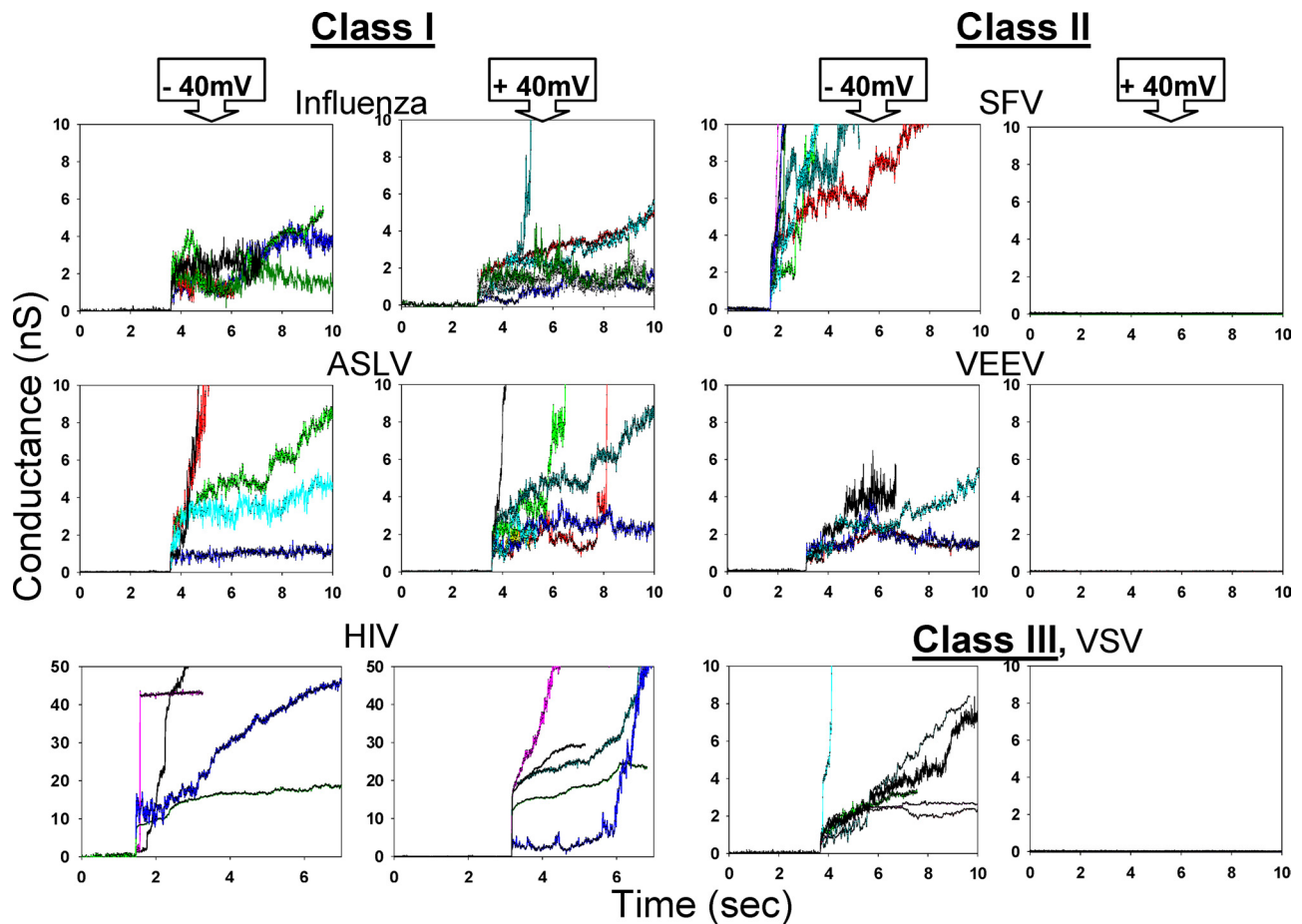
Figure 1. Cell–cell fusion is independent of voltage for class I but voltage dependent for class II and III fusion proteins. For influenza HA at −40 mV, fusion was observed in five of eight experiments (5/8) and at +40 mV, fusion occurred in 7 of 11 experiments. For the other two class I proteins, the number of fusion events per number of experiments were 5 of 7 at −40 mV and 7 of 10 at +40 mV for ASLV Env; 4 of 6 at −40 mV and 5 of 7 at +40 mV for HIV Env. For the class II and class III proteins, fusion pores were observed only at −40 mV. The fraction of cell pairs that fused were 8 of 13 at −40 mV and 0/20 at +40 mV for SFV E1/E2; 4 of 12 at −40 mV and 0 of 11 at +40 mV for VEEV E; and 6 of 9 at −40 mV and 0 of 14 at +40 mV for VSV G. The conductance profiles over time are shown for all observed fusion pores.

voltage across the target cell (Markosyan *et al.*, 2007). This voltage-independence of pore properties can be visually appreciated by comparing the conductance of fusion pores over time at positive and negative potentials (Figure 1, class I).

In the present study, we used the same basic methodologies as previously used for class I proteins to now determine the voltage dependence of fusion for class II and class III viral proteins. To characterize fusion induced by class II proteins, we expressed SFV E1/E2. For SFV E1/E2, fusion occurred for a target cell voltage-clamped at −40 mV, but did not occur for a target cell maintained at +40 mV (Figure 1, class II, SFV), confirming our prior finding (Markosyan *et al.*, 2007). We have now characterized the fusion of effector cells expressing Venezuelan equine encephalitis virus (VEEV) E to target cells as a means of testing the larger question of voltage-dependence as a general principle for class II viral fusion proteins. The fusion of effector cells expressing VEEV E on their surface exhibited voltage dependence similar to that of SFV E1/E2: fusion only proceeded for a transnegative voltage across the target membrane; no pore was observed when a target cell was voltage-clamped to +40 mV (Figure 1, class II, VEEV). Thus, although cell–cell fusion mediated by class I proteins proceeds for both positive and negative voltages,

data so far indicate that positive voltages block fusion in class II proteins.

The three-dimensional structure of one class III fusion protein, VSV G, has been determined, in its initial and final states, by crystallography (Roche *et al.*, 2006; Roche *et al.*, 2007), and we also tested this protein for voltage dependence. As with class II proteins, we found that fusion occurred for transnegative, but not for transpositive, potentials across the target cell. Therefore, although class II and class III viral fusion proteins have different three-dimensional structures, it appears that they share a common functional characteristic in their manner of fusion.

At −40 mV, the percentage of cells that fused was comparable for SFV E1/E2 and VSV G–expressing cells, and both led to considerably more cells fusing than did the VEEV E–expressing cells (see Figure 1 legend for precise numbers), but none of these fusion proteins yielded fusion for target cells voltage-clamped at +40 mV. Because expression levels could be different for the various fusion proteins and different cell types are used as target cells (see *Materials and Methods*) in these systems, the differences in their extents of fusion may not be due to anything intrinsic in their fusion process.
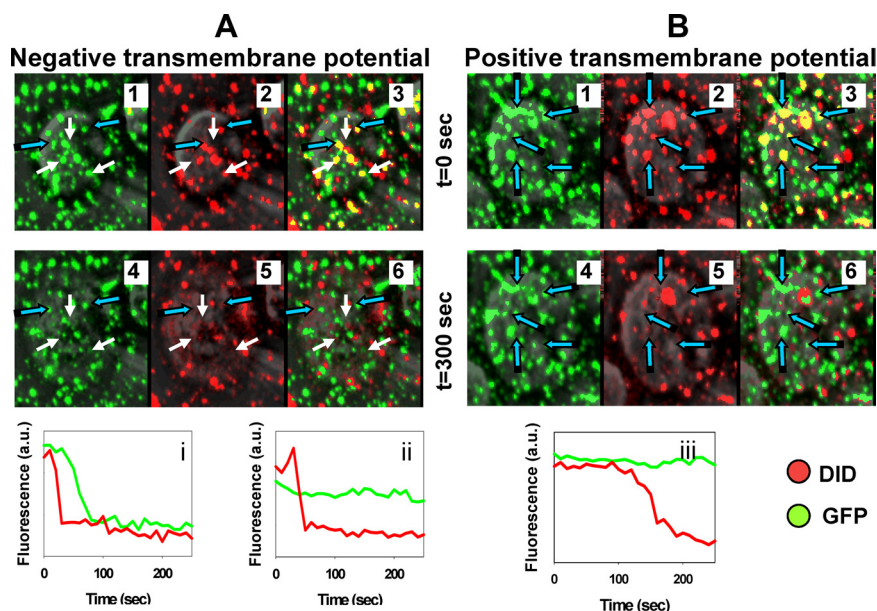
A
Negative transmembrane potential

B
Positive transmembrane potential

Figure 2. Hemifusion and fusion of SFV E1/E2 pseudovirus monitored by dye transfer. (A) Images and traces for −40 mV. Images 1–3 are at t = 0 s, the time fusion was triggered; images 4–6 show the same field of view at t = 300 s. Green punctate spots in images 1 and 4 show GFP within virions; red spots seen in images 2 and 5 are virions labeled by DiD; images 3 and 6 are composites that show both dyes. Selected virions that transfer both dyes are marked by white arrows; those that transfer only DiD are indicated by blue arrows. Trace i illustrates the time course of DiD and GFP fluorescence intensities for virus that fully fuses; trace ii illustrates the time courses for a virus that only hemifuses. (B) Images and traces for +40 mV. The layout of images parallels that of A, but virions are marked by only blue arrows because virions did not fully fuse at +40 mV. Trace iii illustrates that only hemifusion occurs at +40 mV.

Fusion of Individual SFV E1/E2 Pseudotyped Viral Particles to Voltage-clamped Target Cells

We tested whether the voltage-dependency of class II and class III viral-protein–induced cell–cell fusion is also true for the fusion of virus to cell membranes. We used confocal microscopy to follow fusion between pseudovirus and voltage-clamped target cells. The pseudovirus envelope was fluorescently labeled by DiD, and its core was fluorescently marked by GFP (see *Materials and Methods*). To illustrate the general findings, we present experiments using particles pseudotyped with SFV E1/E2 as the fusion protein and then present experiments using VEEV E and VSV G.

After triggering fusion by lowering of pH, for target cells at negative potentials (Figure 2A), a large percentage (~85–90%) of the SFV E1/E2 virions quickly lost DiD. Loss of DiD shows that the envelopes of these virions merged with the plasma membrane of the target cell. A fraction of these hemifused virions also released their GFP (Figure 2A, images 1 and 4, loss of green fluorescence, marked by white arrows), clearly showing that they fully fused to their bound cells. In control experiments, we adhered virus to cover slips and acidified the solution to pH 5.7. Neither DiD nor GFP fluorescence was altered (Supplemental Figure S1), showing that fluorescence decreases observed during fusion experiments are not due to acid-induced quenching of dyes. "Full" fusion is defined as occurring when fusion pores enlarged sufficiently to allow passage of GFP. DiD disappeared from these virions either before or simultaneously with release of GFP. The time delay from triggering fusion until DiD spread for the illustrated virus was ~10 s at −40 mV, and the delay before full fusion was ~20 s (Figure 2A, graph i). The distribution of DiD spread shows that, in general, hemifusion occurred quickly, within a few frames, after triggering fusion (see Figure 5). Some virions that transferred their DiD at negative potentials retained their GFP (several of these virions are marked by blue arrows in images 2 and 5, graph ii). Thus, for negative potentials, some virions fully fused, whereas others did not proceed beyond hemifusion.

In contrast, when a positive potential (+40 mV) was maintained across a target cell membrane, generally lipid dye spread occurred (Figure 2B, images 2 and 5) but GFP failed to transfer (Figure 2B, images 1 and 4, graph iii). We operationally define virions that release DiD but that retain GFP as "hemifused." Some of these virions may have formed pores too small to permit GFP passage, but these pores would be undetected. In the absence of evidence that a small pore has formed, we characterize the DiD spread as hemifusion, the common practice when using lipid and aqueous fluorescent probes to monitor fusion. The percentage of virions that transferred DiD was the same at +40 mV as at −40 mV. We conclude that hemifusion occurs regardless of whether a positive or a negative potential is applied across the membrane of a target cell. Fusion, however, is facilitated by a negative potential and depressed by a positive potential. This is the same pattern observed for cell–cell fusion (Figure 1; Markosyan *et al.*, 2007). The fact that full fusion is voltage-dependent but hemifusion is relatively voltage-independent demonstrates that there is a voltage-dependent step downstream of hemifusion.

Voltage Dependence of Class II and Class III Fusion Proteins in Pseudotyped Virus

We tested whether the voltage dependence of fusion exhibited by SFV E1/E2 pseudotyped virus extends to other class II viral proteins and/or to class III proteins. We performed experiments using the same protocol as for SFV E1/E2, retaining the same GFP-labeled core and DiD labeling, except that the envelope was pseudotyped with VEEV E or VSV G. For both class II proteins SFV E1/E2 and VEEV E and the class III protein VSV G, dependence of fusion on voltage polarity was found to be the same as for fusion between cells (Figure 1): fusion was much more likely for a negative than a positive potential across the target cell (Figure 3, black bars). Spread of DiD from virus to cell occurred for either polarity of voltage across the target cell (hatched bars). For all three fusion proteins, about one-third of the virions that transferred DiD also released GFP. That is, about one-third of the virions that hemifused at −40 mV went on to fully fuse. These results strongly imply that the voltage dependence originally discovered for SFV E1/E2 (Samsonov *et al.*, 2002; Markosyan *et al.*, 2007) is a general phenomenon
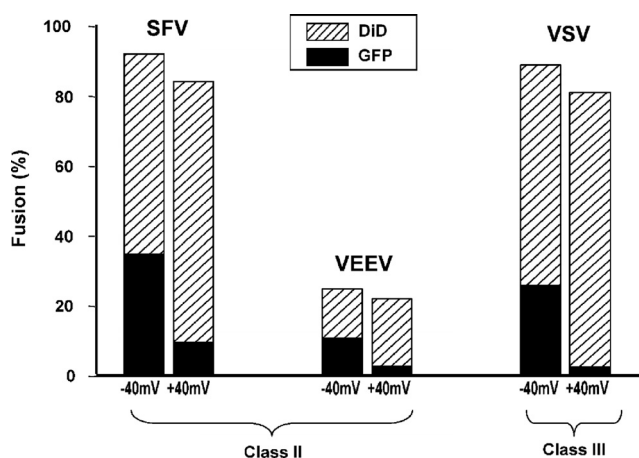
Figure 3. Fraction of pseudovirions that transferred DiD (hatched bars) and GFP (black bars) at −40 and +40 mV.

Figure 4. Time between DiD spread (T_H) and loss of GFP (T_F). The panels provide the distribution of $T_F − T_H$ for virus pseudotyped with each of the three fusion proteins of this study.

that may well hold for all class II and class III viral fusion proteins.

We plotted the distribution time intervals ($T_F − T_H$) between onset of lipid (i.e., DiD) mixing (T_H) and content (GFP) mixing (T_F) for the three types of virions that fused to a cell voltage-clamped at −40 mV. The most commonly observed event for each of the three fusion proteins was the almost simultaneous onset of lipid and content release (Figure 4). A relatively small percentage of the events showed an appreciable delay between DiD and GFP movement. We conclude that when full fusion occurs, the transition from hemifusion usually follows quickly.

Hemifusion States Created by Negative and Positive Potentials

We compared the hemifusion state created as a result of positive and negative voltages in two ways: analysis of the times until hemifusion and analysis of the time course for lipid dye to leave a hemifused virus. For the first comparison, we used a χ^2 analysis (applying Holm-Bonferroni to account for multicomparison tests; see *Materials and Methods*) to determine if the distribution for onset of lipid dye spread was statistically the same at +40 and −40 mV for hemifused virions (Figure 5). (To aid visual appreciation of differences in histograms of Figure 5, the data are replotted as probability density functions in Supplemental Figure S2. Means of the distributions are indicated by the vertical lines, and the SDs are illustrated by the lengths of the horizontal lines.) For each type of virion (SFV, VEEV, and VSV), the time distributions for hemifusion were statistically different at −40 than at +40 mV (confidence level, $p < 0.000005$). The finding that hemifusion occurred more rapidly at −40 than at +40 mV for each of the pseudotyped virions demonstrates that the occurrence of hemifusion is affected by the polarity of membrane potential. The results imply that even though hemifusion occurs for either polarity, the time course of some reconfigurations before hemifusion is voltage-dependent.

We also used a χ^2 analysis to determine whether the time course for the onset of dye spread for virions that hemifused was the same as for virions that fully fused (Figure 5). For target cells held at −40 mV, the onset of dye spread was clearly different for virions that fused than for those that only hemifused ($p < 0.000005$). At +40 mV, the null hypothesis that the time courses were the same for hemifused and
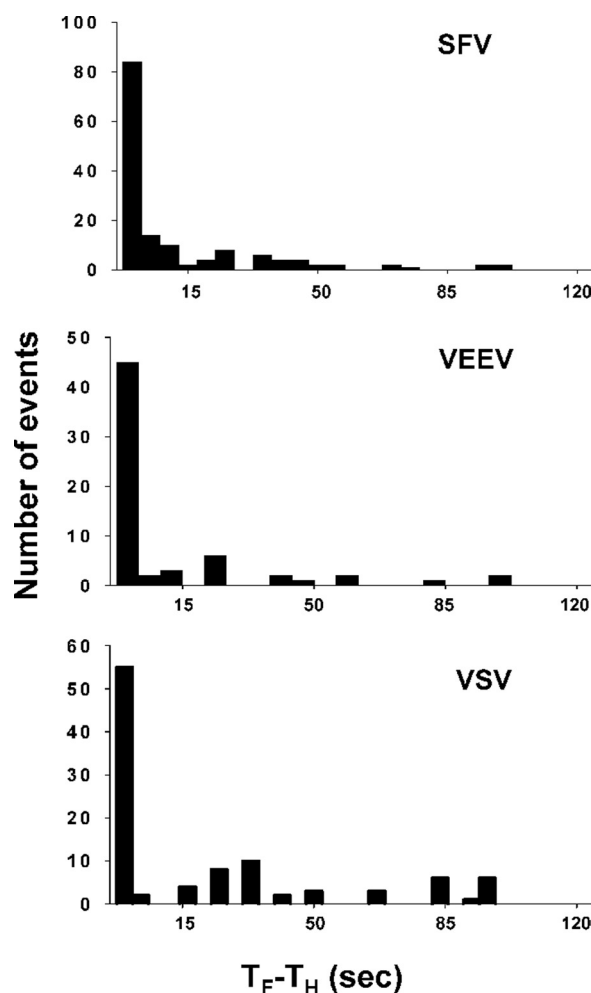
fused cells could not be statistically rejected for SFV and VEEV at a $p = 0.05$ threshold. For VSV, however, the null hypothesis could be rejected. Based on these analyses, we conclude that 1) at the physiologically relevant negative potentials, the time course for onset of lipid merger depends on whether virions only hemifuse or fully fuse and 2) a positive potential eliminates this difference. Lastly, a χ^2 analysis was applied to determine whether the time courses of lipid dye spread for virions that fused depended on voltage polarity. The distributions were clearly different at −40 than at +40 mV for SFV ($p < 0.0003$) and VSV (0.0009). But for VEEV, the distributions were not statistically different at a $p = 0.05$ threshold. Fusion was, however, less likely for the VEEV pseudotype than for the other two fusion proteins, and so here the data set was small, making a statistical analysis less reliable. Placing greater weight on the much larger amount of data available for SFV and VSV (Figure 5), we conclude that the time course for creating the lipid continuity that leads to full fusion is voltage-dependent.

In our second group of analyses, we tested whether there were differences in the hemifusion diaphragm created at −40 and +40 mV. We compared the time course of lipid efflux through the diaphragms by measuring the fluorescence intensity of an individual virion (that only hemifused) over time and collecting all records under the same condi-
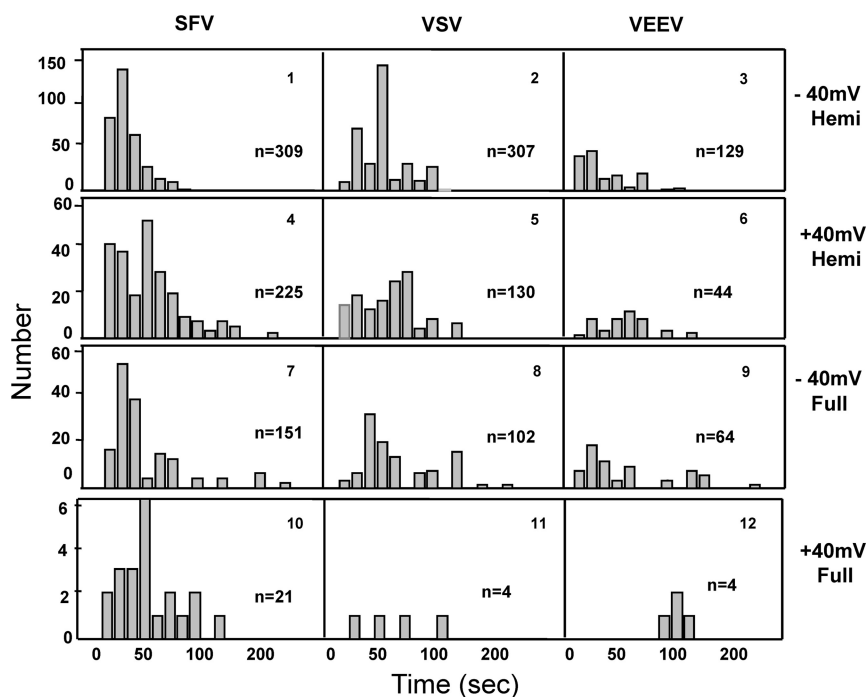
Figure 5. The time distribution for the onset of DiD transfer. First row, distributions at −40 mV for virions that only hemifuse. Second row, distributions for hemifused virions at +40 mV. Third row, distributions at −40 mV for virions that fully fused. Fourth row, distributions for fully fused virions at +40 mV.

tions. For −40 mV, once DiD began to spread, it almost always did so uninterruptedly, until all dye had been released (inset of Figure 6A for a typical record and Supplemental Figure S3A for a panel of many records for SFV E1/E2; inset of Figure 6B, Supplemental Figure S3B for VEEV E; Figure 6C, Supplemental Figure S3C for VSV G). In contrast, at +40 mV the fluorescence profile began to decrease but almost always (~80% of the time for each of the three fusion proteins) stabilized at an intensity well above background. The plateauing of fluorescence shows that lipid dye spread ceased before total transfer. The complete transfer of lipid dye at −40 mV but only partial transfer at +40 mV (Supplemental Figure S4) provides unambiguous evidence that the hemifusion diaphragm is altered by voltage. The mechanism for the plateau in fluorescence at +40 mV that we consider most likely is that the hemifusion process halts and the virus and cell revert back into two distinct membranes. Once they do, lipid continuity is broken and lipid dye transfer can no longer continue. This explanation accounts for the plateau in fluorescence intensity. For the relatively few cases in which DiD release was not complete (i.e., DiD fluorescence exhibited a plateau above baseline) at −40 mV (n = 35 for SFV E1/E2, n = 20 for VEEV E, and n = 25 for VSV G), GFP transfer never occurred. The finding that lipid continuity must be maintained in order for fusion to proceed provides strong evidence that hemifusion is an intermediate of full fusion.

The differences in lipid dye spread for the two voltages are apparent not only from individual records, but also from profiles of fluorescence intensity obtained by averaging individual virion intensities over many virions after aligning the time at which the intensities began to decrease (Figure 6, −40 mV, ●, and +40 mV, ▲). By applying a pairwise t test (with a Holm-Bonferroni correction) for the decreasing fluorescence intensities at each time point, the intensities were statistically distinguishable. More precisely, the null hypothesis that the distributions were the same at the two voltages was rejected for each of the three fusion proteins ($p < 0.05$). That is, the cessation in lipid dye movement was so common

at +40 mV that even averaging fluorescence intensities from individual virions does not obscure the contrast in lipid flux at the two voltages.

The voltage dependent behavior of the three fusion proteins is virtually identical in likelihood of hemifusion and fusion (Figure 3), delay between hemifusion and fusion (Figure 4), times until hemifusion and fusion (Figure 5), and time courses and cessation of lipid transfer through hemifusion diaphragms (Figure 6). This strongly indicates that mechanisms of action are essentially the same for all three proteins. The principles uncovered by detailed characterization of one of these proteins probably generalize to the other two.

Identifying Voltage-dependent Steps Upstream and Downstream of Hemifusion

To identify steps in fusion that utilize membrane potential, we created, for SFV E1/E2, an intermediate stage between hemifusion and fusion. SFV E1/E2–pseudotyped virions were bound to target cells held at −40 mV, and pH was lowered to 5.7 at 12°C, followed by neutralization (at this low temperature) to generate CAS (see *Materials and Methods* and Figure 7, schematic). For almost every virion (>90%), DiD spread immediately upon the creation of CAS, regardless of whether voltage was maintained at −40 mV (Figure 7B, column 2, and see Supplemental Figures S6 for examples in which CAS was held for 8 min rather than 3 min) or switched after creation to +40 mV (Figure 7B, column 4, and Supplemental Figure S5). The demonstration that lipid transfers from virus to cell at CAS provides unambiguous proof that hemifusion has been achieved at CAS. The finding that DiD moved from virus to cell, but GFP always remained within the virion demonstrates that full fusion—a fusion pore that enlarges—has not yet happened. Control experiments showed that fluorescence intensities remained constant if the procedure used to make CAS was followed but the solution was not acidified. This establishes that lipid transfer required lowering of pH. Control experiments also
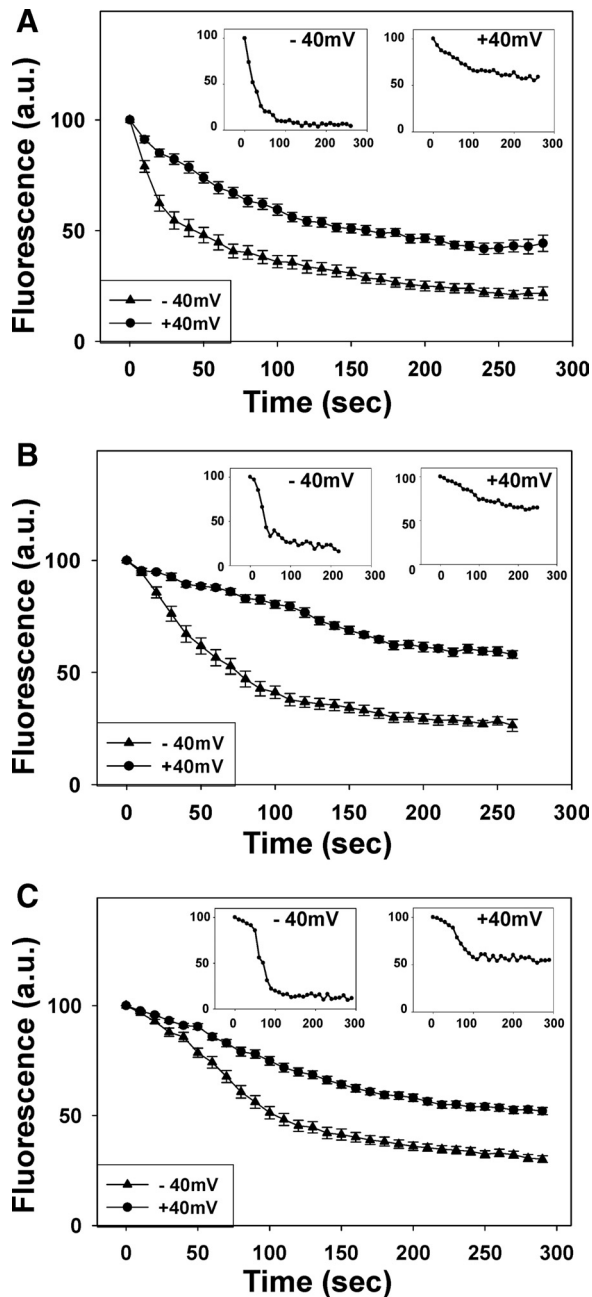
Figure 6. Fluorescence intensity profiles of DiD within hemifused virions pseudotyped with SFV E1/E2 (A), VEEV E (B), and VSV G (C). The average profiles from many virions are shown in the main graphs. Insets, illustrative records from individual virions show that DiD transfer is complete at −40 mV, but at +40 mV generally terminates before all dye leaves the virions. A large number of individual profiles in Supplemental Figures S1 and S2 document that the illustrated profiles are indeed typical.

showed that the addition of CPZ did not alter either DiD or GFP fluorescence (Supplemental Figure S7). As was the case when temperature was always 37°C, DiD continued to move from virus to cell if −40 mV was maintained (Figure 7B, columns 2 and 3; Supplemental Figures S5A, 1 and 2, and S4), but this movement tended to cease if the target cell was held at +40 mV (at the low temperature) after CAS (Figure 7B, column 4; Supplemental Figure S5B). As was the case for hemifusion at 37°C, the most likely explanation for the pla-

teaus of fluorescence intensity at +40 mV is that the state of hemifusion is not irreversible—it can be routed back to separate membranes. A positive membrane potential across the target cell promotes this reversal.

Raising temperature at CAS to 37°C at a negative potential led to appreciable fusion (Figure 7A, column 2), albeit less than the control (lowering pH at 37°C for a negative potential, column 1). This provides extremely strong evidence that the state of hemifusion reached at CAS is a bona fide, functionally active intermediate on the path to fusion: temperature was raised at neutral pH, and thus additional (i.e., "bystander") copies of SFV E1/E2 could not have undergone low pH–induced conformational changes that would lead to the formation of new hemifusion diaphragms. It is formally possible that low pH–activated fusion proteins that had not participated previously in hemifusion could have induced fusion when temperature was raised, but the small contact area between a virus and a cell membrane makes this unlikely. Individual records show that virions that transferred GFP upon raising temperature also exhibited a spurt in DiD spread (Figure 7B, column 2, right). The augmented DiD spread is consistent with the expectation that lipid more readily flows through a fusion pore than through a hemifusion diaphragm. For virions that did not fully fuse upon raising temperature (i.e., GFP did not transfer), the flux of DiD was not altered. Individual and average fluorescence profiles for the two cases show that before the temperature increase, DiD transferred faster for virions that did not fuse upon raising temperature. This was the case even when CAS was sustained for a long time (8 rather than 3 min) before raising temperature (Figure 8; Supplemental Figure S4, A and B).

It is common practice to conclude that cell membranes are in a state of hemifusion if the addition of CPZ leads to aqueous content mixing (Melikyan *et al.*, 1997; Chernomordik *et al.*, 1998; Armstrong *et al.*, 2000; Zavorotinskaya *et al.*, 2004). In the present study, we know that the state of hemifusion is functional and thus the pseudovirion-cell system provides an opportunity to check the validity of the standard test for a state of functional hemifusion. Addition of CPZ, while maintaining low temperature, resulted in appreciable release of GFP (Figure 7A, column 3). These virions also exhibited an increased rate of DiD movement (Figure 7B, column 3, right trace). Virions that did not release GFP (left trace for column 3) upon CPZ addition often exhibited more rapid movement of DiD after CPZ addition. The simplest explanation for this increase in DiD flux is that the addition of CPZ induced the formation of fusion pores that did not enlarge sufficiently to permit permeation of GFP. Quantitatively, at CAS ~90% of the virions released DiD; upon addition of CPZ at low temperature, ~20% of the virions transferred GFP, 60% exhibited increased DiD flux without GFP transfer, and 10% were not affected. (The remaining 10% of the virions had not hemifused at CAS.) The finding that an appreciable percentage (~25%) of virions hemifused to a cell released GFP upon addition of CPZ unambiguously shows that a large pore was created. Based on the increase in rate of lipid transfer, a small fusion pore (i.e., one that does not enlarge) formed for a much greater percentage (~65%) of the hemifused virions. If this is correct, the most common consequence of CPZ addition is formation of a small pore that does not enlarge to a size that permits GFP permeation. Enlargement of fusion pores is an energetically unfavorable process (Cohen and Melikyan, 2004; Chernomordik and Kozlov, 2008). The nonenlargement of these CPZ-induced pores and their different patterns of DiD spread provide strong support for the claim
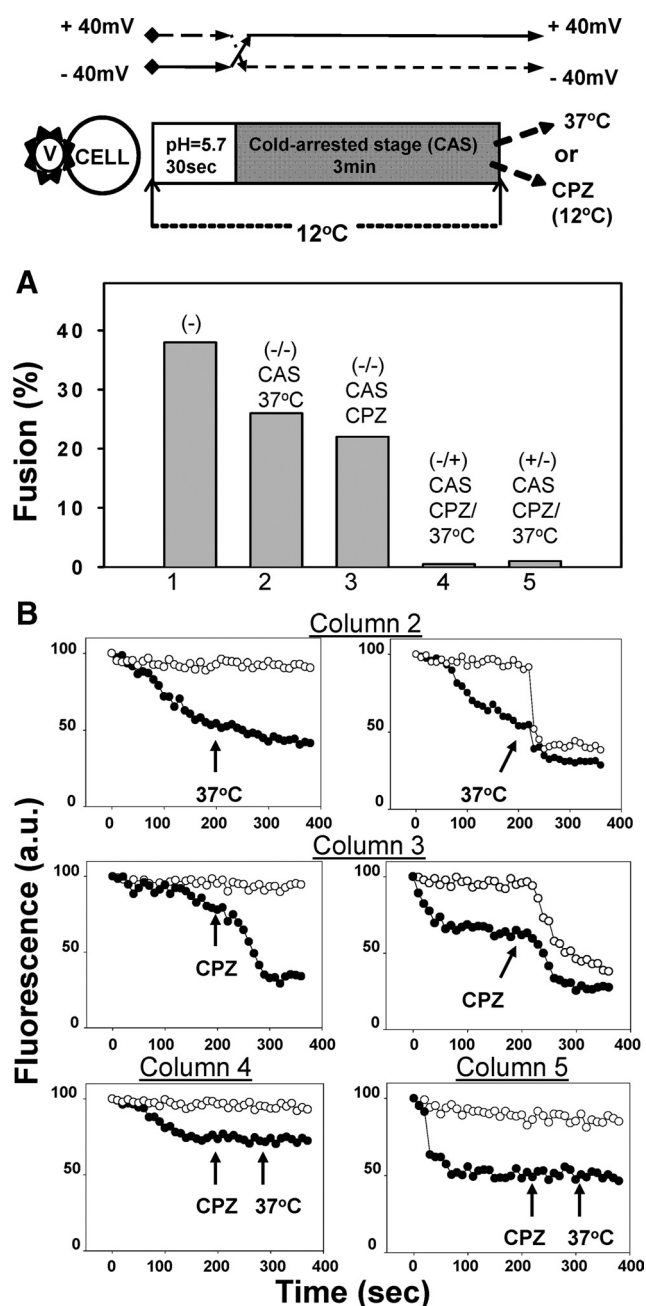
Figure 7. Fusion from CAS for virus pseudotyped with SFV E1/E2. Top, schematic for creating CAS (also see *Materials and Methods*). (A) The voltage polarity used to create CAS is indicated by the sign preceding the diagonal; the polarity after CAS is indicated by the sign that follows the slash. For target cells maintained at −40 mV, raising temperature (3 min after generating CAS) to 37°C led to significant fusion (column 2), albeit somewhat less than if fusion was triggered at 37°C without creating the intermediate (column 1). Adding CPZ 3 min after CAS led to fusion (column 3) comparable in extent to that after raising temperature (column 2). Switching voltage polarity to +40 mV after the 3 min neutralization subsequent to CAS⁻ and immediately adding CPZ led to less fusion (column 4) than that when polarity had not been switched (column 3). Creating CAS for +40 mV across the target cell, immediately (before the 3 min reneutralization) switching polarity to −40 mV, led to little fusion when CPZ was added after the 3-min acidification (column 5). Extents of fusion were quantified by GFP dispersal. (B) Typical records of individual fluorescence profiles for columns of A. (Column 1 is fusion without creating CAS. A typical record of DiD

that reconfiguration of fusion proteins after pore formation is necessary for pore growth. The nonenlargement also indicates that these CPZ-generated pores differ in some way from those naturally produced by fusion proteins. Pores generated by fusion proteins (e.g., upon raising temperature at CAS), almost always enlarge (traces of Figures 7; also Figure 8 below).

The addition of CPZ while holding the target cells at a positive holding potential was ineffective in promoting fusion (Figure 7, A and B, column 4). Inspection of individual records shows that the fluorescence intensity of DiD exhibited a plateau after an initial decrease (Figure 7B, column 4), providing additional support for the conclusion that a positive potential reverses hemifusion. When CAS was created by holding the target cell at a positive potential (rather than a negative potential, as for all other experiments of this figure), and then immediately switching to −40 mV, neither addition of CPZ nor raising temperature caused GFP release (Figure 7A, column 5). Records of DiD spread show a plateau in fluorescence intensity (Figure 7B, column 5; Supplemental Figure S5C), strongly indicating that reversal of hemifusion for a positive potential across the target cell is the reason neither the addition of CPZ nor elevated temperature could then promote fusion. The results of the set of experiments of Figure 7 validate the common use of CPZ in assessing levels of hemifusion. Moreover, the analysis of fluorescence intensity profiles of individual virions has revealed the underlying mechanism that explains why some virions fuse and others do not after CPZ addition.

We assessed the time course for reversal of hemifusion by creating CAS for a negative potential, switching voltage to +40 mV after a 1-min reneutralization and then raising temperature to 37°C at progressively longer times (Figure 8). Increased time after reneutralization led to less fusion: fusion upon immediately raising temperature (Figure 8A, column 1) was greater than that upon raising temperature after 20 s (column 2), which in turn was greater than raising temperature after 2 min (column 3). All levels of fusion were less than when temperature was immediately raised after the 1-min acidification while maintaining the target cell, before and after CAS, at −40 mV (e.g., see Figure 7A, column 1). A plateau in DiD fluorescence was more likely to occur the longer CAS was maintained at +40 mV before raising the temperature (illustrated by individual traces in Figure 8B and Supplemental Figure S6, A and B). A reversal of hemifusion into separate membranes at +40 mV would, as previously argued, account for the plateau in DiD fluorescence and for the loss of fusion activity over time as CAS is maintained.

Endosomal voltages are somewhat smaller than the 40 mV values we routinely used. We therefore determined the dependence of fusion over a range of applied potentials for an individual batch of pseudovirions expressing SFV E1/E2 (Figure 9). The dependence is shallow, changing by one

and GFP transfer is shown in Figure 2; records of DiD transfer in the absence of GFP transfer are presented in Figure 6.) Column 2, DiD continued to transfer after raising temperature, but GFP was retained (left). Upon raising temperature, DiD transfer (●) was transiently boosted and GFP (○) was released (right). Column 3, the addition of CPZ caused the rate of DiD release to greatly increase, but GFP was retained (left). CPZ addition caused DiD flux (●) to increase and GFP (○) to be released (right). Columns 4 and 5, DiD fluorescence plateaus after maintaining +40 mV, and neither addition of CPZ nor raising temperature altered the leveled fluorescence. Column numbers of B correspond to those of A. For all columns, the extents of GFP transfer are shown.
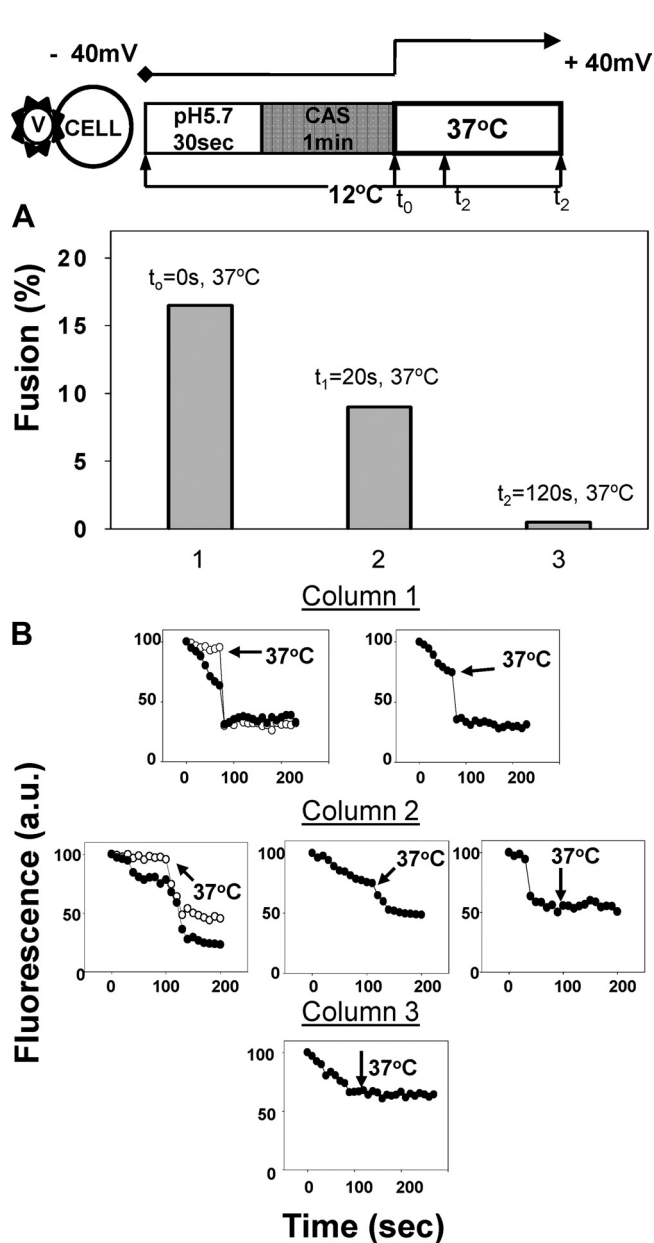
Figure 9. Voltage dependence of fusion for SFV E1/E2 pseudovirus as a function of voltage across a target cell membrane. The graph was obtained for experiments that used a single batch of pseudovirus. A total of 45 virions were analyzed at each indicated voltage and the percentage of virions that fused (i.e., transferred DiD and GFP) was calculated.

exponential (i.e., e-fold) for each 20 mV. Compared with the amount of fusion at −40 mV, ~40% of the virions fused at 0 mV. About +30 mV had to be applied across the target cell membrane in order to completely abolish fusion. Therefore, even small negative potentials, on the order of the 10—20 mV reported for endosomes (Sonawane *et al.*, 2002), aid fusion. Because voltage dependency is shallow and there is at least one voltage-dependent step downstream of hemifusion, it is likely that any particular voltage-dependent step involves the movement of less than one formal charge across the membrane.

DISCUSSION

SFV E1/E2, VEEV E, and VSV G are typical of their fusion classes, and we chose these fusion proteins because each is routinely used to determine characteristics of its class. Because these proteins are typical, it seems highly probable that voltage dependence is a general property that extends to all class II and III viral fusion proteins, and if so, voltage dependence would likely be regulated by a common structural feature. Because negative voltages are present across endosomal membranes, more efficient fusion for negative voltages could have provided an evolutionary advantage to those virions that utilized voltage. Moreover, this advantage would have contributed to the conservation of the structure that confers voltage dependence.

There are precedents for the necessity of membrane potential in the transfer of endosomal contents into cytosol and in the steps of membrane fusion. Many bacterial toxins that are taken up into endosomes, such as diphtheria toxin (Gordon and Finkelstein, 2001) and tetanus (Hoch *et al.*, 1985; Gambale and Montal, 1988), deposit their lethal (e.g., enzymatic) subunit into cytosol through pores. The formation of these pores, created by other subunits of the toxin, requires low pH and is facilitated by negative potentials across the endosomal membrane. Endosome voltage is thus utilized in bacterial infection, and the present study strongly suggests this use of voltage extends to viral infection as well. In fertilization of egg by sperm, positive potentials across the egg membrane cause fusion pores to close (McCulloh and Chambers, 1992); the voltage sensor probably resides in a sperm molecule that inserts into the egg membrane (Iwao and Jaffe, 1989). This voltage dependence of fusion of sperm to egg and location of the voltage

Figure 8. Reduction in fusion over time of holding target cells at +40 mV after CAS. Top, schematic for creating CAS and switching voltage and temperature. (A) Raising temperature to 37°C immediately after switching voltage to +40 mV (column 1) led to about half the fusion obtained if voltage polarity had not been changed (see Figure 7). Less fusion was obtained when temperature was raised at progressively greater times (20 s, column 2; 120 s, column 3) after switching voltage to +40 mV. (B) The possible outcomes at each time of raising temperature are illustrated by typical fluorescence records of individual virions. In all cases, arrow denotes raising temperature to 37°C. Column 1, left record, raising temperature immediately after switching voltage to +40 mV led to both a spurt in decline of DiD fluorescence (●) and transfer of GFP (○). Right record, the temperature increase led to a spurt in DiD flux (●) without GFP transfer (not shown). Column 2, left record, temperature increase induces full fusion as seen by both GFP transfer (○) and an increase in DiD flux; middle record, temperature jump induced greater DiD flux, but GFP did not transfer (not shown); right record; DiD fluorescence intensity had plateaued and temperature jump was without effect. Column 3, fluorescence plateaus before raising temperature, and fluorescence is not affected by temperature increases.
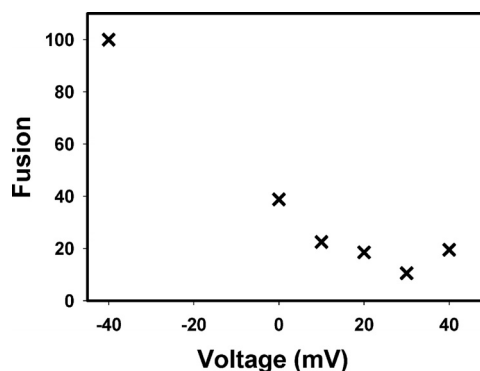
sensor is the same as we have found for fusion mediated by class II and class III viral fusion proteins, with sperm and virus serving analogous roles.

Voltage-dependent Steps Downstream of Fusion

The finding that switching from −40 to +40 mV after creating CAS reduces fusion clearly demonstrates that there are voltage-dependent steps downstream of hemifusion (Figure 7, column 4). Mechanistically, the reversal of hemifused membranes to separate membranes accounts for the voltage dependence downstream of hemifusion. Many intermediate states of full fusion, including hemifusion and the initial fusion pore, are expected to be able to either revert to their immediate upstream state or to continue to progress to a downstream state. In cell–cell fusion, a state of hemifusion can reverse (Gaudin, 2000; Leikina and Chernomordik, 2000; Giraudo et al., 2005). Our records of lipid dye movement from individual virions that show incomplete transfer (Figures 7–9 and supplemental figures) directly demonstrates that hemifusion can reverse to preceding states as part of the normal fusion process. For class II and class III viral proteins, the membrane potential across the target membrane controls the probability that hemifusion reverses to separate membranes or continues on to full fusion.

Hemifusion as an Intermediate of Full Fusion

Is hemifusion an intermediate of full fusion? This has been a fundamental and long-standing question in the fields of viral and eukaryotic fusion. There is no question that hemifusion can occur, as many examples have been demonstrated (Kemble et al., 1993; Melikyan et al., 1995b, 2000b; Chernomordik et al., 1998; Giraudo et al., 2005; Reese et al., 2005; Yoon et al., 2006; Subramanian and Geraghty, 2007; Schwartz and Merz, 2009; Wang et al., 2009). However, in the case of fusion between two biological membranes, it has proved difficult to show that hemifusion occurs naturally as an intermediate on the way to full fusion. Many experimental manipulations have been derived to attempt to unambiguously demonstrate and/or capture states of hemifusion, but the roundabout conditions that have been needed to carry out these experiments in biological systems have generally led to states of hemifusion that have been end states or part of a side pathway. Two prior studies using virus expressing class I proteins (Melikyan et al., 2005; Floyd et al., 2008) show that movement of lipid between membranes precedes the creation of a fusion pore. Results using indirect means—addition of CPZ and/or exogenous lipids that alter membrane curvature—have previously provided evidence that fusion induced by class II and class III viral proteins also proceeds through hemifusion (Gaudin, 2000; Zaitseva et al., 2005). The combination of evidence—DiD spread preceding GFP transfer for fusion at 37°C, spread of lipid dye without GFP release at CAS, faster DiD spread (in the absence of GFP transfer) induced by addition of CPZ at CAS, and promotion of GFP transfer by the addition of CPZ, all shown for individual virions—makes it unlikely that the spread of DiD and retention of GFP are always consequences of the presence of small fusion pores and never the result of hemifusion. Furthermore, our finding that viral contents do not transfer if lipid continuity is disrupted at the physiological membrane potential of −40 mV provides another new line of evidence that hemifusion is necessary for fusion to proceed. The findings of the present study thus strongly bolster the hypothesis that hemifusion is a bona fide intermediate of fusion for class II and class III viral proteins.

The fact that lipid transfer is slower for hemifused virions that proceed to fusion than it is for those that do not is reminiscent of the pattern of lipid spread for fusion between red blood cells and eukaryotic cells expressing the fusion protein of influenza virus. In the latter case, there is strong evidence that lipid does not transfer at all for states of hemifusion that proceed to full fusion (Chernomordik et al., 1998). It was proposed that the fusion proteins must form a tight "fence" around sites of hemifusion if a fusion pore is to subsequently form (Chernomordik et al., 1998). We propose an alternate explanation: a greater accumulation of fusion proteins around a site of hemifusion increases the probability that a fusion pore forms and, unrelated to the mechanism of pore formation, also reduces lipid transfer. In any case, the difference in the structural feature that does cause the different lipid movements through the hemifusion diaphragm may be a controlling factor in the transition from hemifusion to fusion. The temporal sequence of lipid transfer and pore formation we observe on the same viral particle provides extremely strong experimental evidence that hemifusion is a functional intermediate that proceeds on to full fusion.

The Voltage Sensor

In the natural setting, virions containing class II and class III proteins are triggered to fuse by low pH within endosomes. As a practical matter, it has proven difficult to reliably and quantitatively measure voltages across endosomes, as they are inaccessible to electrodes and cannot be voltage-clamped, but it has been clearly shown that endosomes have negative (i.e., inside-positive) membrane potentials. The most carefully calibrated quantitative measurement we are aware of places the steady-state potential in the range of negative 10–20 mV (Sonawane et al., 2002), which is the polarity we find facilitates fusion in our model systems.

For all classes of viral fusion proteins, multiple copies of a fusion protein act cooperatively to induce fusion (Melikyan et al., 1995a; Plonsky and Zimmerberg, 1996; Markovic et al., 2001; Gibbons et al., 2003; Magnus et al., 2009). Because the measured voltage dependency is a consequence of the movement of charges of the entire array of participating fusion proteins, a single protein contributes less than one formal charge. In the case of SFV E1, it has been shown by electron microscopy that six copies of the fusion protein interact to form a rosette (Gibbons et al., 2003). If this rosette induces fusion, each of the monomers contributes to the total voltage dependence; each of the six proteins would thus provide a small fraction of a formal charge to voltage dependency. In the crystals used to determine three-dimensional structure, it has been found that VSV G organizes into a hexagonal lattice (Roche et al., 2007). So here also, each individual protein contributes a portion of the overall charge movement. It is likely that dipoles associated with amino acids, or perhaps even peptide bonds, rather than charged amino acids, are the sensors.

The three-dimensional structure of VSV G exhibits features of both class I and class II proteins. In common with all class I proteins, it contains a triple stranded coiled-coil in its pre- and postfusion states (Roche et al., 2006). Because class I proteins do not exhibit voltage-dependence, it is unlikely that the region of VSV G that forms the coiled-coil contributes to voltage dependence. VSV G also has domains arranged in a manner somewhat similar to that of class II proteins. Class II proteins consist of three domains, linked via two hinges; VSV G has been assigned four domains (Roche et al., 2007). Low pH induces the three domains of class II proteins to rotate relative to each other around the

two hinges without large-scale conformational changes in any of the domains. For VSV G, low pH causes a similar rotation of two domains (DIII and DIV) around a hinge. Class I fusion proteins do not possess such hinges. If essentially the same mechanism is responsible for the voltage dependence of all class II and class III proteins, domain rotation around hinges may hold the key because there are small loops at the periphery of class II and class III protein domains that insert into membranes as a result of domain rotation (Rey *et al.,* 1995; Lescar *et al.,* 2001; Modis *et al.,* 2003; Roche *et al.,* 2007). We conjecture that portions of these membrane-inserted loops respond to voltage. If this is correct, voltage dependence of fusion mediated by class II and class III proteins would naturally follow as a common feature.

ACKNOWLEDGMENTS

REFERENCES

Armstrong, R. T., Kushnir, A. S., and White, J. M. (2000). The transmembrane domain of influenza hemagglutinin exhibits a stringent length requirement to support the hemifusion to fusion transition. J. Cell Biol. *151,* 425–437.

Backovic, M., Longnecker, R., and Jardetzky, T. S. (2009). Structure of a trimeric variant of the Epstein-Barr virus glycoprotein B. Proc. Natl. Acad. Sci. USA *106,* 2880–2885.

Blight, K. J., McKeating, J. A., Marcotrigiano, J., and Rice, C. M. (2003). Efficient replication of hepatitis C virus genotype 1a RNAs in cell culture. J. Virol. *77,* 3181–3190.

Bressanelli, S., Stiasny, K., Allison, S. L., Stura, E. A., Duquerroy, S., Lescar, J., Heinz, F. X., and Rey, F. A. (2004). Structure of a flavivirus envelope glycoprotein in its low-pH-induced membrane fusion conformation. EMBO J. *23,* 728–738.

Chernomordik, L. V., Frolov, V. A., Leikina, E., Bronk, P., and Zimmerberg, J. (1998). The pathway of membrane fusion catalyzed by influenza hemagglutinin: restriction of lipids, hemifusion, and lipidic fusion pore formation. J. Cell Biol. *140,* 1369–1382.

Chernomordik, L. V., and Kozlov, M. M. (2008). Mechanics of membrane fusion. Nat. Struct. Mol. Biol. *15,* 675–683.

Cohen, F. S., and Melikyan, G. B. (2004). The energetics of membrane fusion from binding, through hemifusion, pore formation, and pore enlargement. J. Membr. Biol. *199,* 1–14.

Connor, R. I., Chen, B. K., Choe, S., and Landau, N. R. (1995). Vpr is required for efficient replication of human immunodeficiency virus type-1 in mononuclear phagocytes. Virology *206,* 935–944.

Floyd, D. L., Ragains, J. R., Skehel, J. J., Harrison, S. C., and van Oijen, A. M. (2008). Single-particle kinetics of influenza virus membrane fusion. Proc. Natl. Acad. Sci. USA *105,* 15382–15387.

Gambale, F., and Montal, M. (1988). Characterization of the channel properties of tetanus toxin in planar lipid bilayers. Biophys. J. *53,* 771–783.

Gaudin, Y. (2000). Rabies virus-induced membrane fusion pathway. J. Cell Biol. *150,* 601–612.

Gibbons, D. L., Erk, I., Reilly, B., Navaza, J., Kielian, M., Rey, F. A., and Lepault, J. (2003). Visualization of the target-membrane-inserted fusion protein of Semliki Forest virus by combined electron microscopy and crystallography. Cell *114,* 573–583.

Gibbons, D. L., Vaney, M. C., Roussel, A., Vigouroux, A., Reilly, B., Lepault, J., Kielian, M., and Rey, F. A. (2004). Conformational change and protein-protein interactions of the fusion protein of Semliki Forest virus. Nature *427,* 320–325.

Giraudo, C. G., Hu, C., You, D., Slovic, A. M., Mosharov, E. V., Sulzer, D., Melia, T. J., and Rothman, J. E. (2005). SNAREs can promote complete fusion and hemifusion as alternative outcomes. J. Cell Biol. *170,* 249–260.

Gordon, M., and Finkelstein, A. (2001). The number of subunits comprising the channel formed by the T domain of diphtheria toxin. J. Gen. Physiol. *118,* 471–480.

Harrison, S. C. (2008). Viral membrane fusion. Nat. Struct. Mol. Biol. *15,* 690–698.

He, J., Choe, S., Walker, R., Di Marzio, P., Morgan, D. O., and Landau, N. R. (1995). Human immunodeficiency virus type 1 viral protein R (Vpr) arrests cells in the G2 phase of the cell cycle by inhibiting p34cdc2 activity. J. Virol. *69,* 6705–6711.

Heldwein, E. E., Lou, H., Bender, F. C., Cohen, G. H., Eisenberg, R. J., and Harrison, S. C. (2006). Crystal structure of glycoprotein B from herpes simplex virus 1. Science *313,* 217–220.

Hoch, D. H., Romero-Mira, M., Ehrlich, B. E., Finkelstein, A., DasGupta, B. R., and Simpson, L. L. (1985). Channels formed by botulinum, tetanus, and diphtheria toxins in planar lipid bilayers: relevance to translocation of proteins across membranes. Proc. Natl. Acad. Sci. USA *82,* 1692–1696.

Iwao, Y., and Jaffe, L. A. (1989). Evidence that the voltage-dependent component in the fertilization process is contributed by the sperm. Dev. Biol. *134,* 446–451.

Kadlec, J., Loureiro, S., Abrescia, N. G., Stuart, D. I., and Jones, I. M. (2008). The postfusion structure of baculovirus gp64 supports a unified view of viral fusion machines. Nat. Struct. Mol. Biol. *15,* 1024–1030.

Kemble, G. W., Henis, Y. I., and White, J. M. (1993). GPI- and transmembrane-anchored influenza hemagglutinin differ in structure and receptor binding activity. J. Cell Biol. *122,* 1253–1265.

Kielian, M., and Rey, F. A. (2006). Virus membrane-fusion proteins: more than one way to make a hairpin. Nat. Rev. Microbiol. *4,* 67–76.

Lamb, R. A., and Jardetzky, T. S. (2007). Structural basis of viral invasion: lessons from paramyxovirus F. Curr. Opin. Struct. Biol. *17,* 427–436.

Leikina, E., and Chernomordik, L. V. (2000). Reversible merger of membranes at the early stage of influenza hemagglutinin-mediated fusion. Mol. Biol. Cell *11,* 2359–2371.

Lescar, J., Roussel, A., Wien, M. W., Navaza, J., Fuller, S. D., Wengler, G., Wengler, G., and Rey, F. A. (2001). The Fusion glycoprotein shell of Semliki Forest virus: an icosahedral assembly primed for fusogenic activation at endosomal pH. Cell *105,* 137–148.

Magnus, C., Rusert, P., Bonhoeffer, S., Trkola, A., and Regoes, R. R. (2009). Estimating the stoichiometry of human immunodeficiency virus entry. J. Virol. *83,* 1523–1531.

Markosyan, R. M., Cohen, F. S., and Melikyan, G. B. (2005). Time-resolved imaging of HIV-1 Env-mediated lipid and content mixing between a single virion and cell membrane. Mol. Biol. Cell *16,* 5502–5513.

Markosyan, R. M., Kielian, M., and Cohen, F. S. (2007). Fusion induced by a class II viral fusion protein, semliki forest virus E1, is dependent on the voltage of the target cell. J. Virol. *81,* 11218–11225.

Markovic, I., Leikina, E., Zhukovsky, M., Zimmerberg, J., and Chernomordik, L. V. (2001). Synchronized activation and refolding of influenza hemagglutinin in multimeric fusion machines. J. Cell Biol. *155,* 833–844.

McCulloh, D. H., and Chambers, E. L. (1992). Fusion of membranes during fertilization. Increases of the sea urchin egg's membrane capacitance and membrane conductance at the site of contact with the sperm. J. Gen. Physiol. *99,* 137–175.

Melikyan, G. B. (2008). Common principles and intermediates of viral protein-mediated fusion: the HIV-1 paradigm. Retrovirology *5,* 111.

Melikyan, G. B., Barnard, R. J., Abrahamyan, L. G., Mothes, W., and Young, J. A. (2005). Imaging individual retroviral fusion events: from hemifusion to pore formation and growth. Proc. Natl. Acad. Sci. USA *102,* 8728–8733.

Melikyan, G. B., Brener, S. A., Ok, D. C., and Cohen, F. S. (1997). Inner but not outer membrane leaflets control the transition from glycosylphosphatidylinositol-anchored influenza hemagglutinin-induced hemifusion to full fusion. J. Cell Biol. *136,* 995–1005.

Melikyan, G. B., Markosyan, R. M., Brener, S. A., Rozenberg, Y., and Cohen, F. S. (2000a). Role of the cytoplasmic tail of ectropic moloney murine leukemia virus Env protein in fusion pore formation. J. Virol. *74,* 447–455.

Melikyan, G. B., Markosyan, R. M., Roth, M. G., and Cohen, F. S. (2000b). A point mutation in the transmembrane domain of the hemagglutinin of influenza virus stabilizes a hemifusion intermediate that can transit to fusion. Mol. Biol. Cell *11,* 3765–3775.

Melikyan, G. B., Niles, W. D., and Cohen, F. S. (1995a). The fusion kinetics of influenza hemagglutinin expressing cells to planar bilayer membranes is affected by HA density and host cell surface. J. Gen. Physiol. *106*, 783–802.

Melikyan, G. B., White, J. M., and Cohen, F. S. (1995b). GPI-anchored influenza hemagglutinin induces hemifusion to both red blood cell and planar bilayer membranes. J. Cell Biol. *131*, 679–691.

Miyauchi, K., Kim, Y., Latinovic, O., Morozov, V., and Melikyan, G. B. (2009). HIV enters cells via endocytosis and dynamin-dependent fusion with endosomes. Cell *137*, 433–444.

Modis, Y., Ogata, S., Clements, D., and Harrison, S. C. (2003). A ligand-binding pocket in the dengue virus envelope glycoprotein. Proc. Natl. Acad. Sci. USA *100*, 6986–6991.

Modis, Y., Ogata, S., Clements, D., and Harrison, S. C. (2004). Structure of the dengue virus envelope protein after membrane fusion. Nature *427*, 313–319.

Plonsky, I., and Zimmerberg, J. (1996). The initial fusion pore induced by baculovirus GP64 is large and forms quickly. J. Cell Biol. *135*, 1831–1839.

Reese, C., Heise, F., and Mayer, A. (2005). Trans-SNARE pairing can precede a hemifusion intermediate in intracellular membrane fusion. Nature *436*, 410–414.

Rey, F. A., Heinz, F. X., Mandl, C., Kunz, C., and Harrison, S. C. (1995). The envelope glycoprotein from tick-borne encephalitis virus at 2 A resolution. Nature *375*, 291–298.

Roche, S., Bressanelli, S., Rey, F. A., and Gaudin, Y. (2006). Crystal structure of the low-pH form of the vesicular stomatitis virus glycoprotein G. Science *313*, 187–191.

Roche, S., Rey, F. A., Gaudin, Y., and Bressanelli, S. (2007). Structure of the prefusion form of the vesicular stomatitis virus glycoprotein G. Science *315*, 843–848.

Samsonov, A. V., Chatterjee, P. K., Razinkov, V. I., Eng, C. H., Kielian, M., and Cohen, F. S. (2002). Effects of membrane potential and sphingolipid structures on fusion of Semliki Forest virus. J. Virol. *76*, 12691–12702.

Schwartz, M. L., and Merz, A. J. (2009). Capture and release of partially zipped trans-SNARE complexes on intact organelles. J. Cell Biol. *185*, 535–549.

Skehel, J. J., and Wiley, D. C. (1998). Coiled coils in both intracellular vesicle and viral membrane fusion. Cell *95*, 871–874.

Sonawane, N. D., Thiagarajah, J. R., and Verkman, A. S. (2002). Chloride concentration in endosomes measured using a ratioable fluorescent Cl- indicator: evidence for chloride accumulation during acidification. J. Biol. Chem. *277*, 5506–5513.

Subramanian, R. P., and Geraghty, R. J. (2007). Herpes simplex virus type 1 mediates fusion through a hemifusion intermediate by sequential activity of glycoproteins D, H, L, and B. Proc. Natl. Acad. Sci. USA *104*, 2903–2908.

Wang, T., Smith, E. A., Chapman, E. R., and Weisshaar, J. C. (2009). Lipid mixing and content release in single-vesicle, SNARE-driven fusion assay with 1–5 ms resolution. Biophys. J. *96*, 4122–4131.

White, J. M., Delos, S. E., Brecher, M., and Schornberg, K. (2008). Structures and mechanisms of viral membrane fusion proteins: multiple variations on a common theme. Crit. Rev. Biochem. Mol. Biol. *43*, 189–219.

Yoon, T. Y., Okumus, B., Zhang, F., Shin, Y. K., and Ha, T. (2006). Multiple intermediates in SNARE-induced membrane fusion. Proc. Natl. Acad. Sci. USA *103*, 19731–19736.

Zaitseva, E., Mittal, A., Griffin, D. E., and Chernomordik, L. V. (2005). Class II fusion protein of alphaviruses drives membrane fusion through the same pathway as class I proteins. J. Cell Biol. *169*, 167–177.

Zavorotinskaya, T., Qian, Z., Franks, J., and Albritton, L. M. (2004). A point mutation in the binding subunit of a retroviral envelope protein arrests virus entry at hemifusion. J. Virol. *78*, 473–481.